

# A compact platform for efficient generation and single-shot measurement of high-field terahertz wave with a broadband naturally synchronized mid-infrared source

Yingying Ding<sup>1,2</sup>, Liwei Song<sup>1,\*</sup>, Junyu Qian<sup>1,2</sup>, Zhe Liu<sup>1</sup>, Pengfei Wang<sup>1,2</sup>, Yanyan Li<sup>1</sup>, Yujie Peng<sup>1</sup>, Ye Tian<sup>1,\*</sup>, and Yuxin Leng<sup>1</sup>

<sup>1</sup> State Key Laboratory of High Field Laser Physics and CAS Center for Excellence in Ultra-intense Laser Science, Shanghai Institute of Optics and Fine Mechanics, Chinese Academy of Sciences, Shanghai 201800, P.R. China

<sup>2</sup> Center of Materials Science and Optoelectronics Engineering, University of Chinese Academy of Sciences, Beijing 100049, P.R. China

Received: 10 June 2020 / Received in final form: 7 October 2020 / Accepted: 8 December 2020

**Abstract.** High-field terahertz (THz) wave is a powerful tool for investigating ultrafast dynamics such as the motion of electrons, the vibration of crystal lattices, the precession of spin, etc. In this letter, we demonstrate the generation of intense single-cycle THz pulses from an organic crystal DSTMS (4-N, N-dimethylamino-4'-N'-methyl-stilbazolium 2,4,6-trimethylbenzenesulfonate) via optical rectification. The generated THz field is characterized by single-shot electro-optic sampling with a linearly chirped probe beam. Meanwhile, the spectrum of the infrared pump is broadened to an octave which supports a 1.9-cycle pulse duration. The proposed scheme displays a sophisticated platform of efficient high-field THz generation, single-shot THz measurement, and a broadband mid-infrared source which is naturally synchronized with the THz pulses.

## 1 Introduction

Terahertz (THz) wave is a special kind of radiation which situates between microwave and infrared and has a wavelength range of 300  $\mu\text{m}$ –3 mm. For a long time, the THz wave has received considerable attention [1] because it resonates with the vibration and rotation of many molecules, and it has the capacity to generate a strong electromagnetic field in a picosecond time scale. The advent of broadband THz pulse has opened an avenue for numerous ultrafast dynamic research, including ultrafast magnetic switching [2] and ultrafast carrier dynamics of semiconductors [3]. More recently, a single-cycle THz pulse with high energy has been extensively used for exploring various responses [4] such as manipulation of antiferromagnetic spin waves [5], field-free orientation and alignment of polar molecules [6], revelation of molecular polarizability anisotropy of liquid water [7], coherent electron manipulation [8], extreme nonlinear phenomena in solids [9], and spin resonance coherent control in antiferromagnetic materials [10].

In the past decades, much effort has been exerted to generate single-cycle intense THz pulses because of its great value in the abovementioned applications. There are several innovative approaches to generate THz wave [11–15], however, some of them are not suitable to be used as the source of THz pump-probe experiments because of

the relatively low efficiency and poor stability. Among the THz generation technologies, optical rectification (OR) in nonlinear crystals driven by infrared laser pulses has been extensively used because of its advantages such as high efficiency and stability, as well as compact optical design [16–18]. The OR process is usually driven by femtosecond infrared laser pulses with a broad bandwidth. Different frequencies of the pump spectrum produce a mixed polarization that emits THz wave. To acquire higher generation efficiency, a phase-matching condition should be fulfilled to allow the difference-frequency generation (DFG). In recent years, the performance of organic crystals, which shows high nonlinear susceptibility, has also been significantly improved with the improvement in the manufacturing technology. Especially with the appearance of novel organic crystal DSTMS (4-N, N-dimethylamino-4'-N'-methyl-stilbazolium 2,4,6-trimethyl-benzenesul-fonate) [19] with a high electro-optic (EO) coefficient and that is well phase-matched at the pump wavelength, a series of advances have been made in the field of intense single-cycle THz pulse generation by OR [20–22]. For THz detection, the electro-optical sampling (EOS) measurement using ZnTe, GaP and other crystals is a common method [23–25]. In this paper, we use the DSTMS crystal for THz generation, and the THz electric field is characterized based on EO effect. Using a chirped femtosecond laser pulse that collinearly propagates with THz pulse, the birefringence changes in the refractive index of the EO crystal induced by the THz electric field can be detected [26,27]. Conventional time-domain electro-optic

\* e-mail: [slw@siom.ac.cn](mailto:slw@siom.ac.cn), [tianye@siom.ac.cn](mailto:tianye@siom.ac.cn)

sampling method [28–30] requires a sequence of repeat sampling to improve the signal-to-noise ratio, and the data is obtained by the continuous collection and integration of signal versus time delays. Obviously, the demand for real-time acquisition of a signal cannot be satisfied by the relatively slow-speed multi-shot signal acquisition method. In our experiment, which is different from traditional time-domain optical measurements, the temporal waveform of the THz pulse is detected using a single-shot pump-probe method based on EO effect with a linearly pre-chirped probe pulse. The proposed method not only greatly reduces the difficulty of system construction with the improvement in measurement accuracy for the real-time profile of THz wave [31,32], but also provides superior data-acquisition speed that can perfectly meet the demand of a low-repetition frequency high-power THz electric field measurement in the future. When a pre-chirped probe pulse synchronously passes through an EO crystal with a THz pulse, the direction of polarization of different frequency components in the probe pulse will be changed to a specific degree that is proportionate to the original THz electric field to be measured. The spectrum of the pre-chirped probe pulse completely and synchronously records the temporal waveform of the original THz field, which allows the perfect transformation from a polarization modulation of the chirped probe pulse into a spectrum amplitude modulation with the help of polarization selection, differential numerical simulation of spectrum and spectrometer, and, lastly, realization of a real-time characterization.

In the processes of OR, spectral broadening of the pump pulse also occurs. Thus, a strong THz platform which THz pulse is naturally synchronized with the broadband mid-infrared pulse is set up. Based on this compact platform, significant research in diverse fields could be carried out. For example, the changes induced by intense THz pulse of infrared absorption spectrum of water can be studied [33], the coherent THz control of antiferromagnetic spin waves can be detected by mid-infrared pulses [34], the generation of high harmonics in solids can be realized by the destruction of solid lattice symmetry caused by strong THz field [35], and so on.

## 2 Experimental set up

In this study, the principle of THz generation is based on OR processes, which induces a steady state of polarization. Unlike other nonlinear processes, OR process does not change the frequency content of an electric field because the polarization effects it produces are time-independent. THz radiation mainly depends on the DFG process, however instead of having only two frequencies in the original electric field, as a matter of fact, the pump pulse comprises different frequencies. The generation of a THz pulse from an organic crystal through OR processes can be explained with the DFG process.

The generated THz frequency is the frequency difference of the two components of the pump infrared beam:  $\omega_{\text{THz}} = \omega_1 - \omega_2$ , where  $\omega_1$  and  $\omega_2$  are frequencies of the pump pulses and  $\omega_{\text{THz}}$  is THz frequency. The formula

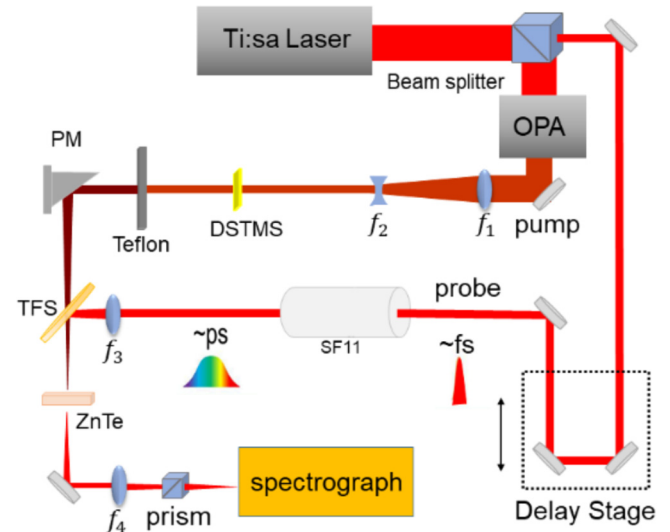


**Fig. 1.** Experimental device for THz generation and detection. Teflon, Teflon plate; PM, parabolic mirror; TFS, thin-film spectroscop; prism, Glan-laser polarizer;  $f_1$ ,  $f_2$ ,  $f_3$  and  $f_4$ , lenses.

theoretically predicts the frequencies generated through the DFG process. According to the spectrum of the pump pulse, the effective spectral range is from 1400 to 1500 nm, and the corresponding frequency ranges from 200 to 214.29 THz. Hence, the theoretical bandwidth is 14.29 THz. However, in practice, the frequency bandwidth of THz pulses that are generated through OR is also limited by the phase match condition and material absorption [19].

As shown in Figure 1, a 640- $\mu\text{m}$  thick DSTMS crystal is pumped by an infrared laser pulse from an optical parametric amplifier with 100- $\mu\text{J}$  pulse energy, 60-fs pulse duration, and 1450-nm central wavelength [36]. The pump beam is down-collimated to a 3-mm diameter and is normally incident to the crystal. Advantages such as high nonlinear susceptibility (with nonlinear optical coefficient  $d_{111} = 214 \pm 20$  pm/V) for OR, low absorption coefficient ( $\alpha < 0.7\text{cm}^{-1}$ ) at the pump pulse (approximately 1.45  $\mu\text{m}$ ) and great birefringence effect (with birefringence coefficient  $\Delta n = 0.5$ ) [37] differentiate DSTMS from other crystals.

## 3 Results and discussions

### 3.1 Influences of the incident pulses in the DSTMS crystal

The spectrum bandwidth of the infrared beam expands over a range 1200–2100 nm (measured by NIR Quest 512, Ocean Optics Inc.) and supports 10.6-fs full width at half maximum Fourier limited pulses, as shown in Figure 2. The spectrum broadening in DSTMS crystal is due to the phase-mismatched cascaded nonlinear interaction which consists of mismatched second harmonic generation, frequency back conversion and Kerr-like nonlinear effect [38].

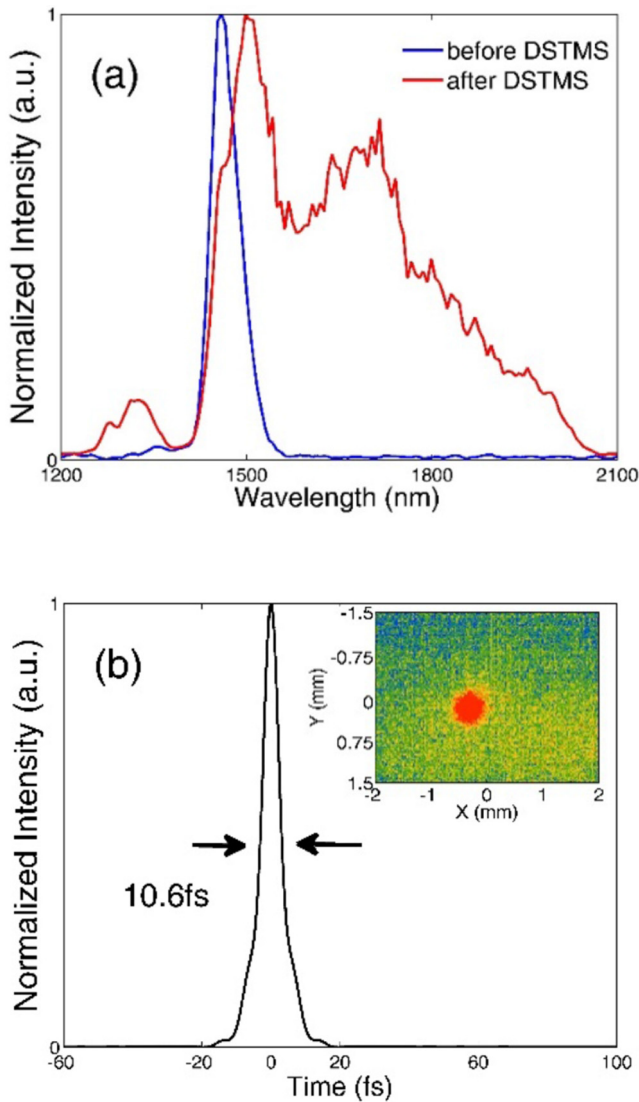


**Fig. 2.** (a) Spectrum prior (blue curve) and subsequent to (red curve) the DSTMS crystal; (b) Fourier transform limited pulse of spectrum broadened by DSTMS crystal (black curve) and THz beam profile measured by a THz CCD (Rigi S2, Swiss Terahertz Inc.) at focus of parabolic mirror with a 2-inch focal length (inset).

### 3.2 Measurement of THz electric field

For measurement of the generated THz waveform, an optical probe beam is linearly chirped for 5.4 ps (from 750 to 850 nm) by passing through a 200-mm long SF11 glass cylinder and then focused collinearly with the THz beam into a 500- $\mu\text{m}$  thick  $\langle 110 \rangle$  ZnTe crystal. The differences of the linearly chirped probe beam spectrum can precisely capture the temporal waveform of the THz beam without moving the delay line. The delay line has a time-scaling function as well as an application for time adjustment within an acquisition window for the position of generated THz pulses. On this basis, the time delay line can ensure the acquisition of THz signal. Based on the Pockels effect, the polarization of a probe pulse that is linearly chirped with

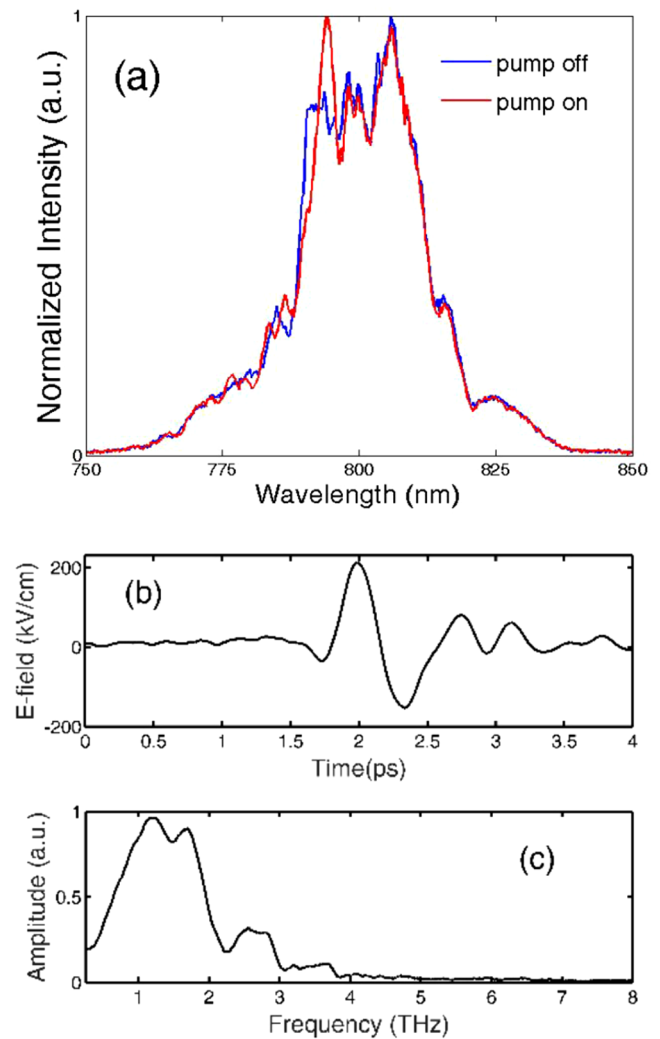


**Fig. 3.** (a) Spectrum of the probe pulse with (red) and without (blue) THz pump pulses; (b) THz electric field. (c) THz spectrum.

different frequencies will change by varying degrees when it is propagating along with a THz pulse in a ZnTe crystal. The direction and angle of these changes are proportional to the co-propagated THz pulse amplitude and phase. It is effortless to analyze these changes in polarization by observing the modulation of the spectrum amplitude on a linearly chirped probe beam through the spectrograph. The phase and amplitude of the instantaneous THz electric field waveform are obtained by analyzing the changes in the probe spectrum (measured by USB4000, Ocean Optics Inc.). The difference in the probe spectrum owing to THz pulse induction is shown in Figure 3a. The temporal waveform of the THz electric field is reconstructed from the differential spectrum distribution (Fig. 3b) and the THz spectrum is also calculated (Fig. 3c).

### 3.3 Calculation of THz electric field

The calculated peak value of the generated THz field is approximately 220 kV/cm, which is based on the

following formula:

$$E_{\text{THz}} = \frac{\lambda_0 \sin(\Delta I/I)}{2\pi n_0^3 r_{41} t L}$$

with EO coefficient  $r_{41} = 0.88$  pm/V [37], which refers to the EO coefficient of ZnTe crystal at the probe wavelength  $\lambda_0 = 800$  nm. Here,  $n_0$ ,  $t$  and  $L$  are the refractive index, transmissivity and thickness of the ZnTe crystal, respectively.  $I$  refers to the intensity of the probe light without THz, with the effect of THz electric field, obvious changes could be observed in the linearly chirped probe laser spectrum (Fig. 3a) and are represented by  $\Delta I$ .

According to the following formula:

$$P = \frac{1}{2} c \epsilon_0 E^2,$$

where  $c$  refers to the velocity of light,  $\epsilon_0$  refers to permittivity of vacuum,  $E$  refers to the peak value of THz electric field, the power density of THz field is calculated with the value of  $6.43 \times 10^{11}$  W/m<sup>2</sup>. The focal spot radius of THz is 0.45 mm and the pulse width is 0.8 ps, thus the THz energy is 0.33  $\mu$ J. In addition, with a THz power meter (3A-P-THz, Ophir Inc.), the average THz power was measured at the value of 340  $\mu$ W with a frequency of 1 kHz at the actual focus, corresponding to a pulse energy of 0.34  $\mu$ J.

## 4 Conclusions

In conclusion, we demonstrate the generation of single-cycle THz pulses through the OR process from a novel organic crystal DSTMS pumped by a broadband infrared pulse (centered at 1.45  $\mu$ m). The probe pulse is linearly chirped by passing through a high dispersion SF11 glass cylinder and then the generated THz electric field modulation in the spectrum is completely recorded by a spectrometer. We obtain the full temporal waveform of the THz field without using any mechanical time-delay device, an approach that is different from traditional detection methods. Not only can this convenient technique simplify the system and reduce the difficulty in detection, but it also greatly improves the speed of signal acquisition, providing an effective routine for real-time analysis of information. Moreover, we observe obvious spectral broadening of pump pulses subsequent to their passing through the DSTMS crystal which is naturally synchronized with the intense THz pulses. In this way, a series of pump-probe research can be carried out by using high-field THz pulses as the pump, combining with the broadband mid-infrared pulse for detection on this platform. We have set up an optimized and compact platform with a multitude of possible applications in mind wherein efficient THz generation and single-shot measurement of intense THz pulse have been demonstrated. In the future, we anticipate achieving few-cycle mid-infrared pulses from the broadband spectrum. In a word, an ultrafast THz-mid-infrared pump-probe experiment platform is demonstrated in this study.

## Author contribution statement

Yingying Ding built the experiment platform and data acquisition as well as writing the original draft of the manuscript. Liwei Song and Ye Tian inspired the work, made the contribution to analytical and numerical calculation, and co-wrote the manuscript. Junyu Qian, Zhe Liu, Pengfei Wang, Yanyan Li, Yujie Peng and Yuxin Leng provided the pump and probe light source.

## References

1. X.C. Zhang, A. Shkurinov, Y. Zhang, *Nature Photon.* **11**, 16 (2017)
2. C. Vicario, C. Ruchert, F. Ardana-Lamas, P.M. Derlet, B. Tudu, J. Luning, C.P. Hauri, *Nature Photon.* **7**, 720 (2013)
3. J. Hebling, M.C. Hoffmann, H.Y. Hwang, K.L. Yeh, K.A. Nelson, *Phys. Rev. B* **81**, 5 (2010)
4. T. Kampfrath, K. Tanaka, K.A. Nelson, *Nature Photon.* **7**, 680 (2013)
5. T. Kampfrath, A. Sell, G. Klatt, A. Pashkin, S. Mahrlein, T. Dekorsy, M. Wolf, M. Fiebig, A. Leitenstorfer, R. Huber, *Nature Photon.* **5**, 31 (2011)
6. S. Fleischer, Y. Zhou, R.W. Field, K.A. Nelson, *Phys. Rev. Lett.* **107**, 5 (2011)
7. P. Zalden, L.W. Song, X.J. Wu, H.Y. Huang, F. Ahr, O.D. Mucke, J. Reichert, M. Thorwart, P.K. Mishra, R. Welsch, R. Santra, F.X. Kartner, C. Bressler, *Nat. Commun.* **9**, 7 (2018)
8. K. Yoshioka, I. Katayama, Y. Minami, M. Kitajima, S. Yoshida, H. Shigekawa, J. Takeda, *Nature Photon.* **10**, 762 (2016)
9. C. Vicario, M. Shalaby, C. P. Hauri, *Phys. Rev. Lett.* **118**, 5 (2017)
10. Z.M. Jin, Z. Mics, G.H. Ma, Z.X. Cheng, M. Bonn, D. Turchinovich, *Phys. Rev. B* **87**, 5 (2013)
11. K.Y. Kim, J.H. Glowina, A.J. Taylor, G. Rodriguez, *Opt. Express* **15**, 4577 (2007)
12. M. Clerici, M. Peccianti, B.E. Schmidt, L. Caspani, M. Shalaby, M. Giguere, A. Lotti, A. Couairon, F. Legare, T. Ozaki, D. Faccio, R. Morandotti, *Phys. Rev. Lett.* **110**, 5 (2013)
13. Y. Tian, J.S. Liu, Y.F. Bai, S.Y. Zhou, H.Y. Sun, W.W. Liu, J.Y. Zhao, R.X. Li, Z.Z. Xu, *Nature Photon.* **11**, 242 (2017)
14. L.L. Du, S.F. Zhao, X.X. Zhou, Z.X. Zhao, *Chin. Phys. B* **24**, 5 (2015)
15. K.Y. Kim, Report No. DOE-UMCP-10706 United States 10. 2172/1253089 CHO English, (2016)
16. J. Hebling, A.G. Stepanov, G. Almaasi, B. Bartal, J. Kuhl, *Appl. Phys. B* **78**, 593 (2004)
17. H. Hirori, A. Doi, F. Blanchard, K. Tanaka, *Appl. Phys. Lett.* **98**, 3 (2011)
18. J.A. Fulop, Z. Ollmann, C. Lombosi, C. Skrobol, S. Klingebiel, L. Palfalvi, F. Krausz, S. Karsch, J. Hebling, *Opt. Express* **22**, 20155 (2014)
19. L. Mutter, F.D.J. Brunner, Z. Yang, M. Jazbinsek, P. Gunter, *J. Opt. Soc. Am. B: Opt. Phys.* **24**, 2556 (2007)
20. C. Vicario, A.V. Ovchinnikov, S.I. Ashitkov, M.B. Agranat, V.E. Fortov, C.P. Hauri, *Opt. Lett.* **39**, 6632 (2014)
21. C. Vicario, B. Monoszalai, C.P. Hauri, *Phys. Rev. Lett.* **112**, 5 (2014)

22. C.P. Hauri, C. Ruchert, C. Vicario, F. Ardana, Appl. Phys. Lett. **99**, 3 (2011)
23. Q. Wu, X.C. Zhang, IEEE J. Sel. Top. Quantum Electron. **2**, 693 (1996)
24. R.A. Lewis, J. Phys. D: Appl. Phys. **52**, 23 (2019)
25. K. Liu, J.Z. Xu, X.C. Zhang, Appl. Phys. Lett. **85**, 863 (2004)
26. B. Yellampalle, K.Y. Kim, G. Rodriguez, J.H. Glowina, A.J. Taylor, Opt. Express **15**, 1376 (2007)
27. M. Kobayashi, Y. Minami, C.L. Johnson, P.D. Salmans, N.R. Ellsworth, J. Takeda, J.A. Johnson, I. Katayama, Sci. Rep. **6**, 6 (2016)
28. Z.G. Lu, P. Campbell, X.C. Zhang, Appl. Phys. Lett. **71**, 593 (1997)
29. Q. Wu, X.C. Zhang, Appl. Phys. Lett. **67**, 3523 (1995)
30. A. Nahata, A.S. Weling, T.F. Heinz, Appl. Phys. Lett. **69**, 2321 (1996)
31. Z.P. Jiang, X.C. Zhang, Appl. Phys. Lett. **72**, 1945 (1998)
32. I. Wilke, A.M. MacLeod, W.A. Gillespie, G. Berden, G.M.H. Knippels, A.F.G. van der Meer, Phys. Rev. Lett. **88**, 4 (2002)
33. F. Novelli, B. Guchhait, M. Havenith, Materials **13**, 15 (2020)
34. K. Tobias, A. Sell, G. Klatt, A. Pashkin, S. Mährlein, T. Dekorsy, M. Wolf, M. Fiebig, A. Leitenstorfer, R. Huber, Nature Photon. **5**, 31 (2010)
35. A.H. Hassan, K. Sergey, T. Klaas-Jan, B. Mischa, M. Gensch, T. Dmitry, Adv. Opt. Mater. **8**, 1900771 (2020)
36. P.F. Wang, B.J. Shao, H.P. Su, X.L. Lv, Y.Y. Li, Y.J. Peng, Y.X. Leng, High Power Laser Sci. Eng. **7**, 5 (2019)
37. C. Vicario, C. Ruchert, F.L. Ardana, C.P. Hauri, in *Terahertz Technology and Applications V*, edited by L.P. Sadwick, C.M. Osullivan (Spie-Int Soc Optical Engineering, Bellingham, 2012)
38. A. Trisorio, M. Divall, B. Monoszlai, C. Vicario, C.P. Hauri, Opt. Lett. **39**, 2660 (2014)

**Cite this article as:** Yingying Ding, Liwei Song, Junyu Qian, Zhe Liu, Pengfei Wang, Yanyan Li, Yujie Peng, Ye Tian, Yuxin Leng, A compact platform for efficient generation and single-shot measurement of high-field terahertz wave with a broadband naturally synchronized mid-infrared source, Eur. Phys. J. Appl. Phys. **93**, 10501 (2021)